Conceptual Study of a Liquid-Core Nuclear Rocket

SEYMOUR T. NELSON,* JERRY GREY,† AND PETER M. WILLIAMS‡
Princeton University, Princeton, N. J.

The liquid-core reactor concept relieves the temperature limitation associated with solid reactors by utilizing liquid-phase fissionable fuel in the highest-temperature portions of the reactor. Such a reactor is composed of a number of cylindrical "fuel elements," each of which consists of an outer region of solid fuel-moderator mixture and an inner layer of the same mixture in the molten phase. Containment of the liquid within the core is achieved by rotation of the fuel elements. The propellant gas is introduced radially inward through perforations in each element, bubbling through the hot, molten-fuel annulus and exhausting axially to the nozzle. The performance potential and feasibility of this concept are examined with regard to nucleonics, heat transfer, bubble hydrodynamics, and vapor entrainment. A current experimental program designed to evaluate certain of the basic assumptions is briefly described. It is concluded that the multielement liquid-core nuclear rocket appears to be feasible. It should provide specific-impulse values upward of 1500 sec, at thrust/weight ratios of the order of unity, with far more practicable design requirements than have been indicated by the single-element configurations of other investigators.

Nomenclature

A_i = cross-sectional area of central cavity in each fuel element, ft²
A_w = surface area of central cavity in each fuel element, ft²
a = equivalent bubble radius [$(\frac{4}{3})\pi a^3$ = bubble volume], ft
C_D = drag coefficient
c_p = specific heat at constant pressure, Btu/lb-°F
d = dilution ratio, number density of ZrC per molecule of UC_2; also used as diameter of radial perforations in fuel elements, ft
f = friction factor
g = local acceleration, ft/sec² or earth gravities
g_0 = force-mass conversion factor, 32.2 ft/sec²
h = total thickness of fuel-mixture cylinder, liquid plus solid, ft
I_{sp_H} = specific impulse of pure hydrogen, real-gas expansion, sec
I_{sp_m} = specific impulse of mixture of gas and vapor, sec
k = thermal conductivity, Btu-ft/ft²-sec-°F
l = thickness of liquid layer, ft
$\dot{m}$ = mass flow rate, lb/sec
M = mean molecular weight of mixture
M_x = molecular weight of component x
N = number of fuel elements; also function defined in text
P = local pressure, psf
P_x = actual vapor pressure of component x over the fuel mixture, psf
P_x^0 = vapor pressure of pure component x, psf
$\mathcal{P}$ = power density, Btu/ft³-sec or Mw/ft³
Q = heat-transfer rate to one bubble, Btu/sec
R = gas constant, ft-lb/lb-°F
Re = Reynolds number
r = bubble radius of curvature, ft
$\mathcal{R}$ = radial coordinate, ft
r_i = radius of liquid-solid interface of fuel element, ft
r_t = aluminum shroud radius, ft
s_y = one-half yield strength of aluminum shroud, psf
T = temperature, °K
T_c = temperature at center of spherical bubble, °K
T_{ic} = initial temperature at center of spherical bubble, °K
T_s = temperature at surface of spherical bubble, °K
t = time, sec
u = bubble velocity, fps
V = $T_s - T_{ic}$
v = $T - T_{ic}$
v_c = $T_c - T_{ic}$
v_r = tangential velocity of propellant in fuel element, fps
X_b = bubble volume fraction
X_x = mole fraction of component X in vapor over fuel mixture
α = $k/\rho c_p$
ΔT = temperature rise, °F
μ = viscosity of liquid, poises or lb/ft-sec
ρ = density of liquid, lb/ft³
ρ_{Al} = density of aluminum shroud, lb/ft
σ = surface tension of liquid, lb/ft
τ = aluminum shroud thickness, ft
θ = aximuthal coordinate of bubble, rad
ω = angular velocity, rad/sec

Subscripts

0 = conditions in nozzle plenum
2 = aft (exhaust) end of fuel-element central cavity
g = gas
m = maximum bubble size

Introduction

THE idea of a liquid-core nuclear rocket was first published by McCarthy[1] in 1954, but essentially no further effort was devoted to the concept until quite recently. McCarthy's original suggestion embodied a single hollow cylinder in which the molten fissionable material would be contained by the centrifugal force developed through rotation of the cylinder. The propellant gas would be injected radially from outside through radial holes in the cylinder, and would be heated by bubbling inward through the molten fuel, finally reaching the hollow central cavity and being exhausted axially down this cavity to a conventional nozzle located at one end of the cylinder.

The McCarthy configuration was recently studied in detail by the present authors and independently by Barrett.[2] Barrett calculated critical masses and dimensions of the hollow cylindrical core, the heat transfer to the propellant bubbles, and the effect on performance of loss of fissionable fuel through vaporization. His results indicated that vapor losses limited specific impulse to about 1200 sec, and that the single-cylinder reactor configuration described previously could develop estimated thrust-to-weight ratios ranging from

Presented as Preprint 64-385 at the 1st AIAA Annual Meeting, Washington, D. C., June 29–July 2, 1964; revision received December 28, 1964. Sponsored by Space Nuclear Propulsion Office, NASA, under NASA Grant No. NsG-389.

* Assistant in Research, Department of Aerospace and Mechanical Sciences. Member AIAA.
† Associate Professor, Department of Aerospace and Mechanical Sciences. Associate Fellow Member AIAA.
‡ Research Staff Member, Department of Aerospace and Mechanical Sciences. Member AIAA.

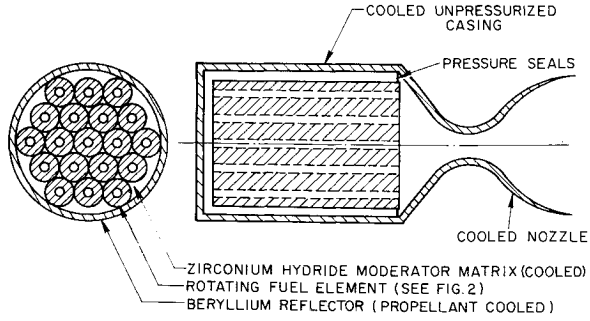

Fig. 1 The multielement liquid-core nuclear rocket.

only 8×10^{-3} (for a 1.5-ft-diam core) to 9×10^{-2} (for a 6-ft core) with required critical masses of uranium-235 ranging between 690 and 10,800 kg, respectively.

Recognition by the present authors of certain objections to the original McCarthy configuration has resulted in several major reorientations of the research program. Consequently, the present liquid-core reactor concept bears little but conceptual resemblance to the system investigated earlier by the authors and by Barrett. In particular, it provides not only a significant increase in specific impulse, but also order-of-magnitude improvements in both attainable thrust-to-weight ratios and critical mass requirements, while removing many of the engineering problems inherent in the McCarthy and Barrett configurations. The primary innovation consists of replacing the large, single hollow cylinder with a number of smaller hollow cylinders (Fig. 1) and has the following significant advantages.

1) The nucleonic efficiency is considerably improved, since the Barrett cavity-type reactor is replaced by what may essentially be treated as a homogenous cylinder.

2) The flow area (the total inner surface area of the cylinders), which is the limiting factor on total propellant flow rate and hence thrust, is considerably increased.

3) The cool interstices between the cylindrical fuel elements can be filled with a good low-temperature neutron moderator, thereby providing a highly efficient thermal neutron spectrum and resulting in a critical mass several orders of magnitude smaller than that of the fast-neutron configuration of Ref. 2.

4) Thermalization of the core permits dilution of the fissionable fuel (e.g., UC_2) by a low-vapor-pressure moderator such as ZrC, thereby mitigating performance degradation due to fuel-element vaporization and improving specific impulse considerably.

5) The entire structure is cool, since the outer portions of each fuel-element cylinder are exposed to the incoming cold propellant; the high-temperature region is therefore limited to the central core of each element, which has no structural function.

6) Rotation of the small cylinders, necessary to retain the molten fuel, is readily achieved in the cool structure by conventional engineering practice.

7) The cool, small-element configuration permits use of high propellant pressures, thus further improving thrust/weight ratio. Moreover, extension to higher chamber pressures is not accompanied by reduced I_{sp} because only a relatively small compensatory increase in propellant stagnation temperature is adequate to offset the higher molecular weight (reduced propellant dissociation) due to the higher pressure. This effect is closely coupled to the decreased loss of vaporized fuel-element material at the higher chamber pressures.

8) The reduced structural loads of the small fuel elements permit the use of a uniform fuel mixture; i.e., the solid part of the hollow fuel-element cylinder can be fabricated from the same material as the part that normally operates in the molten state. This configuration, first suggested by Crocco,[3] eliminates liquid- or solid-phase diffusion between the fissionable fuel mixture and the containing structure, since the containing structure is identical to the molten fuel.

9) The use of multiple elements permits rotation of equal numbers of elements in opposite directions, resulting in zero net angular momentum of both the structure and the exhaust gas.

In the present paper, the nucleonic configuration, the heat transfer from the liquid fuel to the propellant gas, and the vaporization of the molten-fuel mixture are analyzed, and a typical liquid-core nuclear rocket design is presented. In considering the results of this design, it is important to note that the liquid-core nuclear rocket, with a specific impulse of the order of 1500 sec and a thrust-to-weight ratio of the order of unity, not only provides significant performance augmentation in the solid-core range of missions but may even compete with some gaseous-core nuclear rocket concepts.

Reactor and Thrust Chamber Configuration

The multiple-element liquid-core reactor (Fig. 1) consists of a number of rotating "fuel elements," a neutron reflector, a neutron moderator matrix, an unpressurized casing, and an exhaust nozzle. In general appearance, and, in fact, in nucleonic analysis, it closely resembles the configuration of existing solid-core nuclear rocket thrust chambers.

Each fuel element (Fig. 2) is a thick-walled hollow cylinder of UC_2 heavily diluted with ZrC, perforated with many small radial holes for propellant passage and surrounded by a perforated aluminum casing to support the centrifugal load. The cold propellant is introduced through the drive motor shaft into the manifold formed by the perforated aluminum casing, which rotates with the fuel element. The propellant then flows radially inward through the fuel cylinder perforations, in which it is heated to the chamber temperature. When the reactor is started, after propellant flow has been initiated, the inner surface of each element begins to melt, and the solid-liquid interface moves outward in the fuel cylinder until equilibrium is established. The propellant gas then issues from the perforations still remaining in the solid outer part of the fuel cylinder, bubbles radially inward through the molten inner part, and flows axially down the central cavity to the nozzle. Note that, with this design, each element is pressurized to full chamber pressure (plus the required injection pressure drop) but that the reflector and casing are unpressurized.

A good low-temperature moderator such as zirconium hydride (ZrH_2) fills the interstitial spaces between the elements and supports the downstream seal and radial bearings, which carry no thrust load and negligibly small radial load. In the sample design, a 4-in.-thick beryllium reflector containing control drums of conventional design is used on the lateral and upstream core surfaces.

Each fuel element is driven separately, requiring only sufficient power to overcome friction and provide the propel-

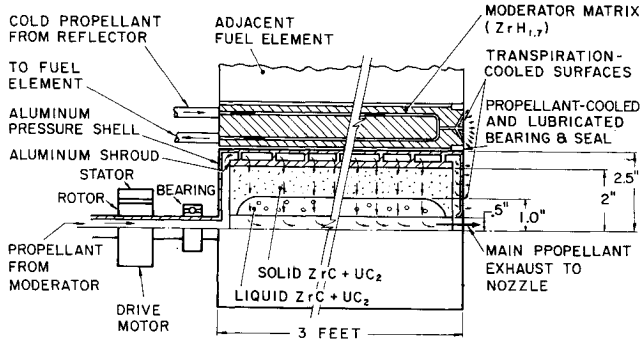

Fig. 2 Typical fuel element for multielement liquid-core reactor.

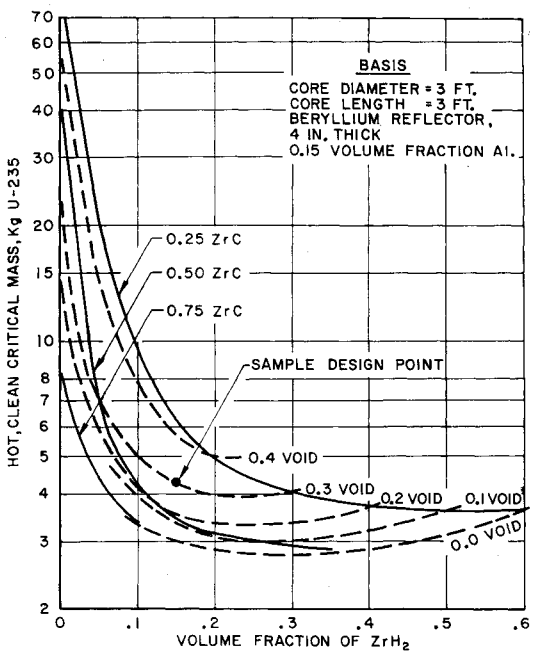

Fig. 3 Effect of core composition on critical mass near design point.

lant with the necessary angular momentum. The thrust load is carried by the upstream bearing, which is cooled by the incoming cold propellant. Typical fuel-element dimensions (not optimized) are shown in Fig. 2.

In normal operation, the incoming H_2 is first used to regeneratively cool the nozzle, the reflector, and the ZrH_2 moderator, and then enters the fuel-element casings at about 100°K. It is heated approximately up to the melting point of ZrC (~3500°K) as it flows radially inward through the perforations in the solid outer portion of the fuel cylinder and then to the sample design chamber temperature of about 4800°K as it bubbles through the inner (molten) portion of the cylinder. The liquid region, therefore, becomes in effect a "topping" device for the addition of heat to the propellant after it has received most of its energy in the solid portion of the fuel element. Note that the exact location of the solid-liquid interface is of little consequence, since the cold incoming H_2 will keep it sufficiently far from the outer surface of the fuel cylinder to maintain structural integrity.

Shutdown of the reactor is accomplished by rotating the reflector control drums until the core becomes subcritical but maintaining propellant flow rate until the molten portion of the fuel elements "freezes in" around channels of flowing hydrogen. Observation of the "freezing-in" of flow channels in liquid metals at normal earth gravity has been reported.[2] Although these channels probably will not resemble the original perforations, they should provide adequate flow area for restart, since any "hot spots" will only cause localized melting on start-up and thus not affect either structural integrity or operation of the reactor. Further consideration of transient behavior is beyond the scope of this paper.

Analysis

Neutronics

Parametric neutronic analyses were made in the vicinity of the reference design dimensions and with the inclusion of interstitial ZrH_2 after earlier computation[4] had shown that excessively high critical masses and large reactor dimensions were required when only carbide moderators were considered. Figure 3 summarizes the analysis for the reference design and shows that, when the ZrH_2 fraction is reduced below about 0.15, the critical mass rises sharply, and little further reduction in critical mass is achieved with greater ZrH_2 fractions. Three-group, two-region computations were made using the WHY code[5] on an IBM 1620 computer. Fast and epithermal constants were taken from data compiled by Deutsch[6] for convenient exploratory calculations of hydrogenous reactors. The computed values of critical mass are for a clean, hot reactor without provision for uranium loss by vaporization. As will be discussed later, the actual initial fuel loading is mission-dependent but is typically about twice that of the critical masses given in Fig. 3.

Propellant Mass Flow Rate

Although the bulk of the heat transfer to the H_2 occurs in the solid portions of the fuel elements, the limits on both mass flow rate and heat transfer are set by the liquid-phase region. Detailed analyses of the characteristics of high-gravity bubble flow[4] are reviewed here, together with pertinent results of a preliminary 1-g experimental study.[7]

In order to maximize the flow rate (and hence the thrust), it is necessary to deal with "large" bubbles. On the other hand, heat transfer is improved with smaller bubbles. It was established analytically,[4] as will be shown later, that flow rate rather than heat transfer is the principal limitation, and therefore attention is confined to large bubbles or, more precisely, to bubbles of high Reynolds number. The regimes of classical 1-g bubble flow are illustrated in terms of empirically observed bubble velocity[8] in Fig. 4. It is implied by these data that the desired regime is that of "spherical-cap" bubbles. As Re is increased past the range over which spherical-cap bubbles appear, the bubbles become unstable, and fragmentation begins to occur. This, of course, still represents a potentially useful regime for the liquid-core reactor, provided that the more violent surface-shattering effect does not contribute to loss of liquid fuel by the mechanism of droplet entrainment. However, in the interest of conservatism as well as amenability to at least approximate analysis, it will be assumed that spherical-cap bubbles represent the maximum-flow condition, and the flow and heat-transfer estimates of the present paper are based on this assumption.

The terminal velocity of a spherical-cap bubble is given by[9] $u = \frac{2}{3}(rg)^{1/2}$. Taking into account the interesting fact that all spherical-cap bubbles, regardless of size, are observed to subtend a half-angle of approximately 52° and noting that $r = 2.179a$, as may readily be shown,[4] we may express the terminal velocity in terms of the "equivalent radius," $u \approx (ag)^{1/2}$. The average mass flow rate of propellant gas per unit liquid surface area is thus

$$\dot{m}/A_w = X_b u \rho_g \approx X_b \rho_g (ag)^{1/2}$$

At the inner surface, the gas density is given by the equation of state, and thus

$$\dot{m}/A_w \approx X_b P_0 (ag)^{1/2}/RT_0$$

Maximization of $\dot{m}/A_w$, and therefore thrust, thus requires that we select the maximum practical values for bubble (void) fraction X_b, chamber pressure P_0, centrifugal acceleration g, and, as indicated earlier, equivalent bubble radius a. From geometrical considerations, i.e., avoidance of bubble interaction at the inner surface, it has been concluded[4] that X_b is limited to about 0.30. Practical values for P_0 are of the order of several hundred atmospheres for the fuel-element design of Fig. 2, and this design also indicates that accelerations of the order of 1000 earth gravities[4] should be readily attainable without introducing structural difficulties.

The maximum equivalent bubble radius is dictated by bubble instability and breakup characteristics, which are rather difficult to predict. However, an order-of-magnitude estimate can be obtained by the simple assumption that the bubble will break up when the local dynamic pressure becomes of the same order as the surface tension. The functional de-

pendence of maximum stable bubble radius should therefore be of the form

$$r_m \sim \sigma/\tfrac{1}{2}\rho u^2$$

Introducing

$$r_m \approx 2a_m \quad \text{and} \quad u \approx (a_m g)^{1/2}$$
$$a_m \approx [(\sigma/\rho)(1/g)]^{1/2}$$

although values of (σ/ρ) are not available for the molten-fuel mixtures under consideration, the surface tension for most refractory metals appears to be about an order of magnitude greater than that of water; it is, therefore, likely that (σ/ρ) will be of the same order as that for water. The significant fact, however, is that the maximum stable bubble radius is dependent on the acceleration g and therefore is subject to the control of the designer. For the selected sample design value of 1000 earth gravities, making the rough assumption that (σ/ρ) is the same as that for water, the maximum equivalent radius of the spherical-cap bubbles in the sample design will be of the order of 1 mm ($\sim$0.040 in.).

To observe the effect of this size limitation on propellant mass flow rate and power density, we introduce the preceding expression for maximum stable bubble radius to obtain

$$\dot{m}/A_w \approx X_b P_0(\sigma g/\rho)^{1/4}/RT_0$$

The liquid property (σ/ρ) is thus comparatively unimportant in limiting the thrust, as is the acceleration g. Clearly, the dominant design variable is the chamber pressure P_0, and the liquid-core rocket is therefore similar to both chemical and solid-core nuclear rockets; i.e., because the maximum propellant temperature is fixed by other considerations (e.g., materials, chemical properties, etc.), the thrust is dictated principally by P_0.

The required power density in the liquid layer of the fuel element may now be estimated for subsequent comparison with the power density permitted by heat-transfer considerations:

$$\mathcal{P} \approx (\dot{m}/A_w)\, c_{p_g}\Delta T_g/l$$
$$\approx (X_b P_0/RT_0 l)c_{p_g}\Delta T_g(a_m g)^{1/2}$$

Taking the average specific heat c_{p_g} of the hot hydrogen at 4 Btu/lb-°F, a temperature rise ΔT_g in the liquid portion of the reactor of 2300°F (1300°C), the thickness l of the liquid layer at 0.5 in., and the other sample design values as given previously, the required liquid-region power density for the sample design is 24,000 Btu/ft^3-sec or about 25 Mw/ft^3.

Heat Transfer

The principal limitation on heat transfer is in the liquid region of the fuel element. This problem has been examined in some detail[4] by considering 1) heat transfer through the liquid boundary layer surrounding the bubble and 2) heating of the gas contained inside the bubble.

Considering first the internal heating of the gas within the bubble, we (conservatively) assume that 1) the spherical-cap bubble is replaced by a spherical bubble of equivalent radius, 2) heat transfer due to convection and radiation inside the bubble is negligible, and 3) the liquid-fuel annulus has a uniform temperature of 4800°K, the inner surface temperature. Assumption 3 is nonconservative, but since the lowest liquid fuel-mixture temperature at the liquid-solid interface is already 3500°K, the degree of nonconservatism represented by this assumption is minor.

The analysis is further simplified by dividing the liquid layer into four annuli of equal thickness, so that each bubble successively traverses the corresponding four concentric regions. The entire problem is thus reduced to four interrelated (but simplified) time-dependent problems of heat conduction into a sphere. Given the liquid fuel and gas temperatures at the solid-liquid interface, as well as the time for traversal of the first annular region, we calculate the temperature at the center of the bubble at the end of this time. Then, taking the new center temperature as an initial value, we calculate the center temperature at the instant the bubble emerges from the second annular region, and so on until it arrives at the inner liquid surface.

The solution to the heat conduction equation with the pertinent boundary conditions has been given by Carslaw and Jaeger[10] as

$$v = \frac{aV}{\mathcal{R}} \sum_{n=0}^{\infty} \operatorname{erfc} \frac{(2n+1)a - \mathcal{R}}{2(\alpha t)^{1/2}} - \operatorname{erfc} \frac{(2n+1)a + \mathcal{R}}{2(\alpha t)^{1/2}}$$

where erfc is the complementary error function

$$\operatorname{erfc} x \equiv \frac{2}{\pi^{1/2}} \int_x^{\infty} e^{-\xi^2}\, d\xi$$

v_c is given by the limit of the preceding as $\mathcal{R} \to 0$:

$$v_c = \frac{aV}{(\pi\alpha t)^{1/2}} \sum_{n=0}^{\infty} \exp\left[-\frac{(2n+1)^2 a^2}{4\alpha t}\right]$$

Traversal times are calculated from bubble velocity formulations given earlier, together with the assumed liquid layer thickness. Variation in bubble size with depth was also taken into account[4] by adjusting the bubble density with the gravity pressure drop and temperature rise of the bubble gases. Results of the calculations for the sample set of conditions gave v_c/V at the end of the first annular region as 0.9944; i.e., over 99% of the total gas temperature rise in each bubble occurs by the time only one-quarter of the liquid layer has been traversed. Thus internal heating of the gas in the bubble is readily accomplished.

We consider now the question of heat transfer across the thermal boundary layer in the liquid surrounding the bubble. The following assumptions are made: The bubble is an undeformed sphere, with $1 \ll Re \ll Re_c$ (Re_c being the critical Reynolds number at which deformation occurs). It moves rectilinearly in a liquid medium, which is effectively infinite, quiescent, and entirely free of surface-active materials. All of the phenomena are steady state. There exists a thermal boundary layer whose minimum thickness is small as compared with the bubble radius. The pressure in the liquid is uniform over dimensions of the order of the bubble size, and μ, ρ, k, and c_p are all very nearly constant. No mass transfer occurs across the interface. On the basis of these assumptions, Nelson[11] has shown that

$$Q = \rho c_p(\Delta T)_j(6\pi\alpha u_j a_j^3)^{1/2} J$$

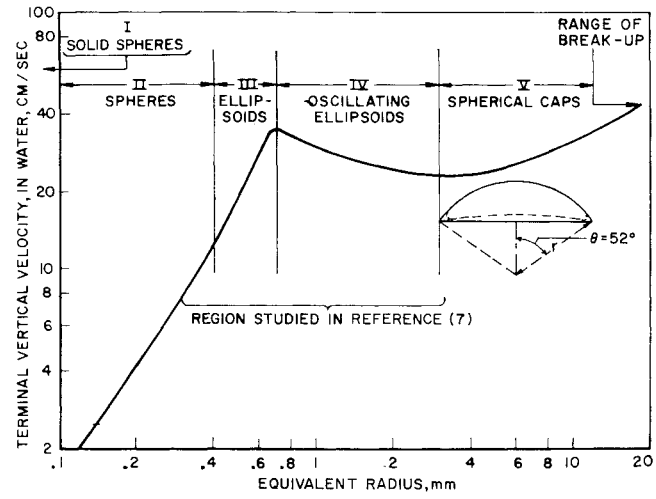

Fig. 4 General regimes of bubble shape and velocity.

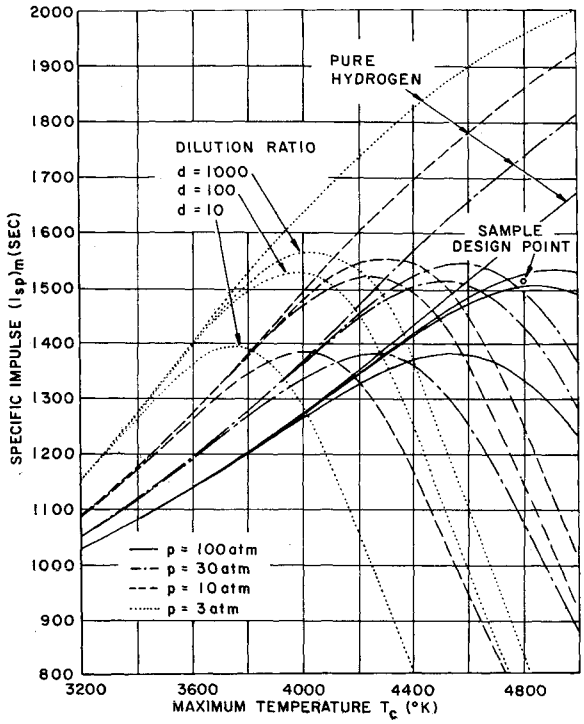

Fig. 5 Specific-impulse optimization of liquid-core nuclear rocket.

where subscript j refers to one annular molten-fuel region; i.e., $j = 1, 2, 3, 4$, and J, which is of the order of π, is given by

$$J = \int_0^{\pi} \frac{\sin^3\theta \{1 - [K(2 + \cos\theta)^{1/2}/(1 + \cos\theta)]\}\, d\theta}{[N^2 - K\{(2 + \cos\theta)^{3/2}(\frac{4}{5}\cos\theta - 2) - \frac{6}{5}(3)^{3/2}\}]^{1/2}}$$

where $N^2 = \frac{2}{3} - \cos\theta + (\cos^3\theta)/3$, $K = (4\,i\,\mathrm{erfc}\theta)/3\,(Re)^{1/2}$, and where $i$erfc is the first integral of the complementary error function, and R_j is based on the bubble diameter $2a_j$. This result may also be expressed in the more familiar form

$$Nu = J\,(3/4\pi)^{1/2} Re^{1/2} Pr^{1/2}$$

Taking estimated values for molten ZrC as follows: $\mu = 10^{-2}$ poise (typical of fused metals), $k = 12$ Btu/hr-ft-°F,[12] and $c_p = 0.1452$ Btu/lb-°F,[13] the attainable heating rate across the boundary layer of a single bubble is $Q = 6.9$ Btu/sec per bubble. Converting this to a volumetric heating rate, the permissible power is $\mathcal{P} = 1.82 \times 10^7$ Btu/ft^3, or 2×10^4 Mw/ft^3. Since this is over two orders of magnitude greater than the energy requirements based on mass flow rate as computed previously, the heat transfer may be considered safely nonlimiting.

Fuel Containment

As in any fluid-core nuclear rocket reactor, one of the principal problems is that of retention of fissionable material within the thrust chamber structure. This is essential, not so much because of the economic penalties due to the high cost of such material, but principally as a result of the severe degradation of specific impulse produced by even small fractions of high-molecular-weight products in the exhaust. In the case of the liquid-core reactor, there are two possible modes of fuel-mixture loss: liquid droplet entrainment by the propellant bubbles as they break through the surface and vaporization of the fuel mixture.

The entrained droplet problem can be readily minimized. Equating centrifugal and axial drag forces, it can be shown for the sample design that the centrifugal force exceeds the drag force by a factor of 10 down to droplet sizes of 0.01 mm. Furthermore, since the length/diameter ratio of the central channel is 36, ample time in the high-g field exists for most of the entrained droplets to "fall" back to the liquid surface.

The evaporation loss is far more severe and, in fact, is directly responsible for the specific-impulse limitation of the liquid-core concept. It is likely that vapor-pressure equilibrium will exist, because the processes of heat conduction and mass diffusion obey the same mathematical relationship, viz., the classical Fourier heat conduction equation, and the boundary conditions for heat conduction are formally identical with those for mass transport.

Under the assumption that vapor-pressure equilibrium exists, a simple analysis can be made. Recall that the fuel is a solution consisting of fissionable material (UC_2) and diluent (ZrC) in the ratio of d moles of the latter per mole of the former. Since both materials are carbides and not grossly dissimilar substances, and since for all of the cases considered $d \gg 1$, we may expect that the molten fuel mixture is a reasonably good approximation to an ideal solution, with UC_2 considered as the solute and ZrC the solvent. Thus

$$P_{UC_2} = P_{UC_2}^{\circ}/(d + 1)$$
$$P_{ZrC} = dP_{ZrC}^{\circ}/(d + 1)$$

and, assuming Dalton's law for the vapor phase, the mole fractions of the various species in the exhaust are

$$X_{UC_2} = P_{UC_2}^{\circ}/P_0\,(d + 1)$$
$$X_{ZrC} = dP_{ZrC}^{\circ}/P_0(d + 1)$$

(The zirconium and carbon vapor equations are sometimes written separately because it is known that ZrC dissociates upon evaporation).

The rocket exhaust thus consists of hydrogen and the preceding mole fractions of fuel-mixture vapor. At a given propellant temperature, therefore, the specific impulse is now downgraded to the value

$$I_{sp_m} = (M_H/M)^{1/2} I_{sp_H}$$

where the mean molecular weight is given by

$$M = \Sigma M_i X_i = \frac{M_{UC_2}}{d+1}\frac{P_{UC_2}^{\circ}}{P_0} + \frac{M_{ZrC}\,d}{d+1}\frac{P_{ZrC}^{\circ}}{P_0} + M_H\frac{P_H}{P_0}$$

In order to determine the dependence of specific impulse on temperature, vapor-pressure data from Ref. 13 were used with the Clausius-Clapeyron equation to calculate the vapor pressures of ZrC and UC_2 at each temperature. The I_{sp_H} and molecular weight (M_H) for pure hydrogen were obtained as functions of P_0 aud T_0 from King's real-gas nozzle calculations[14]; the results are plotted in Fig. 5 for various P_0, T_0, and dilution ratios d.

One further item of interest is the loss rate of fissionable material

$$\dot{m}_{U\text{-}235} = \frac{M_{U\text{-}235}}{M_{UC_2}}\dot{m}_{UC_2} = \frac{\dot{m}}{d+1}\frac{P_{UC_2}^{\circ}}{P_0}\frac{M_{U\text{-}235}}{M}$$

Because of this small but finite loss rate, the dilution ratio in actual operation will vary from the beginning to the end of the mission. However, because the critical-mass requirements are so low, it can be calculated from the preceding that the total fuel loss at specific impulses around 1500 sec will be of the order of the critical mass (~5 kg) for many missions of interest.

Mechanical Design Considerations

Fuel-Element Design

The only high-temperature environments appear at the inner surface of the fuel annulus, where essentially no structural requirement exists, and at the nozzle-end bearing, seal, and fuel-element end-plate. The latter components present the only significant design problem related directly to the fuel elements, and, in fact, will require some ingenuity in pro-

viding adequate hydrogen cooling in the 4800°K, 100-atm nozzle entrance environment. For the present purposes, we assume that these components can be cooled by bleeding cold incoming hydrogen through them directly into the nozzle plenum (Fig. 2). It is not yet possible to determine the extent of performance degradation necessitated by such cooling, should it be necessary. However, nozzle-cooling requirements for the much higher temperatures of gaseous-core rockets have been shown[15] to degrade I_{sp_H} by only 4%; this may be considered as a conservative upper limit for the liquid-core system, which operates at the same pressures but at temperatures a factor of 3 to 4 lower than those discussed in Ref. 15.

One aspect of the centrifugal-field fuel retention technique, discussed at great length by Barrett,[2] and, in fact, used to set his design limitations for the large single-cylinder liquid-core concept, is the effect of the vehicle acceleration field on the shape of the liquid surface. This effect results from the fact that when the vehicle is accelerating in the longitudinal direction, the liquid fuel will be induced to "sag" toward the aft end of each element. However, in the present case, the longitudinal vehicle acceleration is found to be of the order of one earth gravity (thrust/weight ratio of unity), whereas the centrifugal acceleration is of the order of 1000 earth g's. The slope of the liquidus, therefore, will only be of the order of 0.001 rad, or about 0.057°, and the total radial displacement at the aft end of the 3-ft-long element of Fig. 2 will be only of the order of 0.04 in., or about 4% of the innermost diameter of the liquid-fuel annulus of Fig. 2. It is therefore concluded that the effect of longitudinal acceleration is negligible even with the moderate centrifugal fields utilized in the sample design, and thus need not be considered as a limitation on the system.

With regard to stress limitations on the fuel element itself, if we consider that the 5-in.-diam aluminum shroud surrounding the sample design fuel-mixture cylinder of Fig. 2 provides the only support against both the 100-atm propellant pressure and the centrifugal field (i.e., the fuel mixture itself is completely relieved of all load-bearing requirements), the shroud thickness for the postulated sample design speed of 7000 rpm (providing 1000 earth g's at the mid-depth of the liquid layer) is given by

$$\tau = \frac{r_t^2\omega^2 h\rho(1 - h/2r_t)}{g_0 s_y(1 - r_t^2\omega^2\rho_{Al}/g_0 s_y)}$$

or, for the sample design of Fig. 2 with a safety factor of 2, the required Al thickness is $<\frac{1}{4}$ in.

Finally, we must consider the injection pressure loss of the propellant (radial ΔP across the Al shroud and fuel mixture), which consists of friction loss due to flow through the perforations and bubble drag, momentum loss due to heat addition, and gravity head necessary to overcome the high centrifugal field. For the purposes of the present paper, it is sufficient to perform a conservative order-of-magnitude estimate of these losses in order to demonstrate that they are not excessive.

In order to avoid bubble interference until the inner fuel-element surface is broached, the bubble spacing must be at least one bubble diameter on centers, or about 1 mm (~0.040 in.) For the inner fuel liquid-surface diameter of 1 in. and length of 36 in. in the sample design (Fig. 2), the number of perforations per fuel element will be of the order of 80,000, each perforation having a diameter of the order of 0.040 in. and a length of 2 in. The required flow rate is thus 6.5/(42)(80,000) = 1.93×10^{-6} lb/sec per perforation, and the friction pressure loss will be, assuming turbulent flow,[16]

$$\frac{dP}{d\mathfrak{L}} = \frac{2f\dot{m}^2}{g\rho d(\pi d^2/4)^2}$$

The Re is estimated to vary from ~1500 at the tube inlet to ~30 at the tube outlet, so that f will be in the range[16] 0.01 to 0.012. Taking a mean value of 0.011, and a mean value for the propellant density at 100 atm and 1600°K of 0.092 lb/ft^3, the friction pressure drop is less than 1 psi, and the momentum loss due to heating, for the extremely low Mach number flow through the perforations, is of the same order. The gravity loss is only of the order of 5 psi, and therefore the total injection pressure loss is negligible. The injection manifold thus need sustain only slightly higher pressures than the chamber pressure.

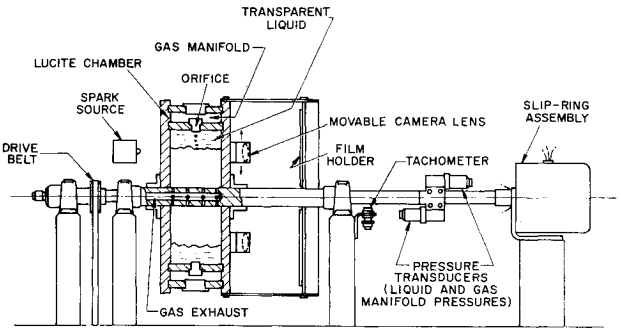

Fig. 6 Apparatus for high-gravity bubble flow studies.

Fuel-Element Drive System

Because each rotating fuel element is a cool, self-contained, pressurized unit, the mechanical drive system does not appear to present any major design difficulties. In the sample design, each of the 43 fuel elements of Fig. 2 is driven at 7000 rpm by a separate turbine or electric motor. High-pressure, cold propellant gas enters the hollow shaft after having been used to cool the moderator matrix, with simple "O"-ring or other low-friction seals available for use in the cool environment.

The power requirements for the element drive motors are those of ordinary mechanical friction and the pumping power necessary to rotate the gas. The former cannot, of course, be estimated at this time, but the pumping power is simply the energy added to the gas to bring it up to 7000 rpm at the ~1-in. radius of the outer liquid surface (the power required to accelerate the gas to 7000 rpm at the 2.5-in. outer fuel-element radius is partly regained as the gas flows radially inward, so that the only residue requiring power input is that still left when the gas leaves the solid part of the fuel element). This residual energy is simply

$$\tfrac{1}{2}\dot{m}v_r^2 = \tfrac{1}{2}(\dot{m}/N)r_i^2\omega = 0.012 \text{ kw per element}$$

and the total rotary pumping power required is only 0.5 kw for the entire reactor. Thus the inherent loading of the drive motors will be essentially that caused by mechanical friction.

Experimental Program

Experimental feasibility studies of the liquid-core concept at Princeton are limited to the fluid flow and heat-transfer aspects of the system. A high-speed double-exposure photographic technique,[7] developed from quantitative measurements of bubble shapes, velocities, and directions of motion, has served to verify the classic 1-g data of Fig. 4 and to demonstrate that the interaction between multiple bubble streams, as compared to the single stream usually studied, is negligible at 1-g. These studies are being extended to high centrifugal fields (~1000g) with the apparatus of Fig. 6, which will provide the same data, together with gross heat-transfer characteristics, in transparent systems (e.g., air bubbles in water). Subsequent studies utilizing low-temperature liquid metals are planned in order to approximate more closely the liquid-core reactor conditions and to establish quantitatively such characteristics as liquid droplet entrainment and coolant passage "freezing-in" on shutdown.

Table 1 Typical design for a multielement liquid-core nuclear rocket

General data		
Specific impulse,[a]		1500 sec
H_2 mass flow		6.5 lb/sec
Uranium loss		0.0012 lb/sec
Chamber pressure		100 atm
Total weight		8000 lb
Reactor core	5000 lb	
Reflector	1000 lb	
Nozzle, pump, motors auxiliary	2000 lb	
Thrust[a]		9750 lbf
Reactor (thermal, reflected type)		
Power level		200 Mw
Core diam, length		3 × 3 ft
Reflector (beryllium)		4 in., rear and sides of core
Fuel elements (see below)		43 rotating cylinders
Coolant		Hydrogen
Moderator		ZrC and ZrH_2
Control		Reflector-mounted control drums, burnable and evaporative poisons

Core composition:

Material	Volume fraction	Weight, lb
ZrC	0.40	3400
ZrH_2	0.15	1100
Al	0.15	500
Void	0.3	
U-235 (clean, hot)		8.8
Final dilution ratio d[a]	850	
Initial dilution ratio d	425	
U-235 burnup[a]	10 g	
U-235 vaporization loss[a]	4 kg	

Fuel element	
Diameter, length	5 in. × 3 ft
Element speed	7000 rpm
Casing material	Aluminum
Interelement matrix	ZrH_2
Inlet coolant temp	100°K
Outlet coolant temp	4800°K
Coolant exit pressure	100 atm
Coolant inlet pressure	100 + atm

Fuel region characteristics:

Region	Solid	Liquid
Material	ZrC	ZrC
Fuel	UC_2	UC_2
Temperatures, °K		
Inlet	100	3300
Outlet	3300	4800
Maximum surface	3500	4800
Power density, Mw/ft³	28.5	25

[a] Mission-dependent; values given are for ΔV = 37,500 fps; payload = 4 tons.

Discussion of Results

In order to illustrate performance of the liquid-core nuclear rocket concept, it was applied to a simple mission consisting of a velocity increment of 37,500 fps and a payload of 4 tons. Characteristics of this sample design, using the general thrust chamber configuration of Fig. 1 and the fuel-element design of Fig. 2, are listed in Table 1, which also includes component weight estimates. The design, based on a specific impulse of 1500 sec, results in a total uranium loss of about 4 kg, or about $50,000. Since the reactor and engine weights as well as the thrust/weight ratio are of the same order as those of the solid-core rocket, the liquid-core rocket can provide nearly double the payload/launch weight of an 800-sec solid-core nuclear rocket. Other characteristics of the system appear in the table.

It has been the object of this paper to describe the liquid-core nuclear rocket in sufficient detail to illustrate the basic physical processes involved and to indicate the major factors affecting performance. It must be pointed out that substantial questions of engineering feasibility remain, prominent among which are 1) problems of bearings for the rotating fuel elements, 2) the failure mode of the reactor when a single fuel element fails, and 3) results of maldistributions of axial liquid thickness, rotation velocity, liquid-solid interface, and flow metering among elements. To some extent these are problems in which portions of the solutions have been demonstrated by existing rotating equipment or nuclear powerplants, and although these problems are significant, they are not believed to offer feasibility barriers to the design.

Conclusions

The multielement liquid-core nuclear rocket of Fig. 1 provides significantly superior performance as compared with the large single-element concept of prior authors.[1, 2] Principal quantitative performance improvements, comparing the sample design of Table 1 with the results of Ref. 2, are 1) increase in I_{sp} from 1200 to 1500 sec, 2) reduction in critical mass of U-235 from the order of 1000 kg to about 5 kg, and 3) increase in thrust/weight ratio from the order of 10^{-2} to unity. The liquid-core nuclear rocket thus parallels quite closely the characteristics of the conventional solid-core system, but with nearly double the specific impulse.

The multielement configuration eliminates essentially all of the high-temperature structural problems and restricts high-pressure regions to the small-diameter fuel elements and the nozzle plenum. The engineering problems of this design appear to be of the same order of difficulty as those of existing solid-core nuclear rocket designs.

It was found analytically that heat transfer to the bubbles in the liquid region of the reactor does not limit the system performance, i.e., the propellant is exhausted at the temperature of the molten-fuel mixture when the limit of mass flow rate has been reached. The mass flow rate, and hence thrust level and power density, depend heavily on (are essentially proportional to) the chamber pressure level, but specific impulse is relatively insensitive to increases in chamber pressure.

References

[1] McCarthy, J., "Nuclear reactors for rockets," Jet Propulsion **24**, 36–37 (1954).

[2] Barrett, W. L., "Liquid-core nuclear rocket," AIAA Paper 64-541 (May 1964).

[3] Crocco, L., "Advanced concepts—introductory remarks," Princeton University Conference on Prospects for Nuclear Aerospace Propulsion, Princeton, N. J. (February 1962).

[4] Nelson, S. T. and Grey, J., "Conceptual design study of a liquid-core nuclear rocket," Princeton Univ. Aeronautical Engineering Rept. 665 (September 1963).

[5] Hunter, C. H. and Hettley, R. A., "WHY, a one-dimensional few-group diffusion code for the IBM 1620," Knolls Atomic Power Lab. Rept. KAPL-M-CT-1, UC-32 (1963).

[6] Deutsch, R. W., "Computing 3-group constants for neutron diffusion," Nucleonics **15**, 47–51 (January 1957).

[7] Lieberherr, J. F., Williams, P. M., and Grey, J., "Bubble motion studies for the liquid core nuclear rocket," Princeton Univ. Aeronautical Engineering Rept. 673 (December 1963).

[8] Haberman, W. L. and Morton, R. K., "An experimental investigation of the drag and shape of air bubbles rising in various liquids," David Taylor Model Basin, Rept. 802 (September 1953).

[9] Moore, D. E., "The rise of a gas bubble in a viscous liquid," J. Fluid Mech. **6**, 113–130 (1959).

[10] Carslaw, H. S. and Jaeger, J. C., *Conduction of Heat in Solids* (Oxford University Press, Oxford, England, 1959), 2nd ed., p. 233.

[11] Nelson, S. T., unpublished memorandum (in preparation).
[12] Tipton, C. R. (ed.), *The Reactor Handbook* (Interscience Publishers, Inc., New York, 1960), 2nd ed., Vol. 1, p. 509.
[13] Juveland, A. C., Deinken, H. P., and Dougherty, J. E., "Loss of zirconium and uranium from fluidized beds of ZrC and UC-ZrC particles at high temperatures," Los Alamos Scientific Lab. Rept. LAMS-2994 (December 1963).
[14] King, C. R., "Compilation of thermodynamic properties and theoretical rocket performance of gaseous hydrogen," NASA TN D-275 (April 1960).
[15] Kramer, E. L. and Gronich, S., "A transpiration-cooled nozzle as applied to a gas-core nuclear propulsion system," J. Spacecraft Rockets **2**, 345–353(1965).
[16] Bonilla, C. F., "Fluid flow in reactor systems," *Nuclear Engineering Handbook*, edited by H. Etherington (McGraw-Hill Book Co., Inc., New York, 1958), pp. 9–33.

MAY-JUNE 1965 J. SPACECRAFT VOL. 2, NO. 3

Collection of Liquid Propellants in Zero Gravity with Electric Fields

J. B. Blackmon*
Douglas Aircraft Company, Inc., Santa Monica, Calif.

Liquid propellants can be collected in a zero-g environment by use of the concept of dielectrophoresis, i.e., the induced motion of electrically neutral bodies in a nonuniform electric field. A brief analysis of the field forces is presented, and liquid collection experiments in simulated and actual zero-g environments are described, including tests in aircraft flying ballistic trajectories. Two dielectrophoretic propellant collection systems for a 250,000-lb liquid-hydrogen/liquid-oxygen space vehicle are described and compared with a typical auxiliary propulsion system for propellant settling. Results indicate that the dielectrophoretic systems are lighter and will provide collecting forces of nearly the same magnitude. The use of the high voltages (10^6 v) required for a dielectrophoretic system on a large vehicle is discussed, and additional applications of the concept are considered. This system appears to offer a lightweight, low-power method of collecting propellant in zero g with forces on the order of 10^{-4}–10^{-2} g. Propellant boiloff losses can be decreased by $\frac{1}{5}$ by collecting the propellant off the tank walls with dielectrophoretic forces.

Nomenclature

b = barometric pressure, cm Hg
T = absolute temperature, °K
E = electric field intensity, v/m
F_v = force/unit volume, newton/m^3
K = dielectric constant
P = pressure, newton/m^2
r_1 = inner electrode radius
r_2 = outer electrode radius
r_3 = tank radius
ϵ_0 = capacitivity of space, farad/m
ρ = mass density, kg/m^3
ρ_e = electric charge density, coul/m^3
σ = conductivity, mho/m
ω = surface free-charge density, coul/m^2
α = surface tension, newton/m

Introduction

TO insure proper engine restart of a liquid rocket in a zero-g environment, a reliable system for orienting the propellant over the tank outlet and providing vapor-free liquid is a necessity. With cryogenic propellants, some means of providing gas venting with no loss of liquid propellant is required, and in some cases the propellants must be continuously supplied to auxiliary systems during zero-g coast phases. We have investigated liquid collection in zero-g environments by dielectrophoresis, which is defined as the induced motion of electrically neutral bodies in a nonuniform electric field. The results of an analysis and some experiments are applied to the design of two hypothetical dielectrophoretic propellant collection systems for a liquid-hydrogen/liquid-oxygen (LH_2/LO_2) space vehicle weighing approximately 250,000 lb. Comparisons with an auxiliary propulsion system suggest that the dielectrophoretic system offers a lightweight, low-power solution. The two systems described consist of thin-walled, cylindrical metal electrodes in the LH_2 and LO_2 tanks with 0.5–1.0 Mv applied. The power dissipated through the liquid propellant by resistance heating is only 0.01–0.05 w. Both systems weigh approximately $\frac{1}{10}$ that of the reference auxiliary propulsion system designed for one restart and 15 vent cycles at 0.01 and 0.001 g, respectively. These systems can also be used to decrease propellant boiloff losses by $\frac{1}{5}$ by positioning the liquid off of the tank walls. Problems associated with the use of high voltages are discussed, and additional applications of the system are considered.

Theory and Analysis

A continuous, dielectric liquid in a nonuniform electric field experiences forces resulting from free charges and from gradients in the field intensity and liquid dielectric constant. The total volume force on a dielectric liquid with no discontinuities in an electric field is[1]

$$\bar{F}_v = \rho_e\bar{E} - (\epsilon_0/2)E^2\nabla K + (\epsilon_0/2)\nabla[E^2\rho(\partial K/\partial\rho)] \quad (1)$$

The first term is the force exerted on free charges, the second term is the force exerted because of inhomogeneity of the liquid, and the last term denotes the dielectrophoretic effect of force on a body in a nonuniform electric field. A rela-

Presented as Preprint 64-265 at the 1st AIAA Annual Meeting, Washington, D. C., June 29–July 2, 1964; revision received November 5, 1964.
* Designer, Advance Propulsion and Power Department, Missile and Space Systems Division.